Retina

A Novel *BEST1* Mutation in Autosomal Recessive Bestrophinopathy

Christopher Seungkyu Lee,[1] Ikhyun Jun,[1–3] Seung-il Choi,[4] Ji Hwan Lee,[1] Min Goo Lee,[2,3] Sung Chul Lee,[1] and Eung Kweon Kim[1,3,4]

[1]The Institute of Vision Research, Department of Ophthalmology, Yonsei University College of Medicine, Seoul, Korea
[2]Department of Pharmacology, Yonsei University College of Medicine, Seoul, Korea
[3]Brain Korea 21 PLUS Project for Medical Sciences, Severance Biomedical Science Institute, Yonsei University College of Medicine, Seoul, Korea
[4]Corneal Dystrophy Research Institute, Yonsei University College of Medicine, Seoul, Korea

PURPOSE. To describe the clinical characteristics associated with a newly identified mutant of autosomal recessive bestrophinopathy (ARB) and confirm the associated physiological functional defects.

METHODS. Two patients with ARB from one family underwent a full ophthalmic examination, including dilated fundus examination, fundus photography, fluorescein angiography, fundus autofluorescence imaging, spectral-domain optical coherence tomography (OCT), electroretinography (ERG), and electrooculography (EOG). Subsequently, genetic analysis for bestrophin-1 (*BEST1*) mutations was conducted through direct Sanger sequencing. The effect of ARB-associated mutations of *BEST1* on the cellular localization was determined by in vitro experiments. Whole-cell patch clamping was conducted to measure the chloride conductance of wild-type *BEST1* and the identified *BEST1* mutants in transfected HEK293T cells.

RESULTS. Two related patients (66-year-old brother and 52-year-old sister) presented with reduced visual acuity and bilateral symmetrical subretinal deposits of hyperautofluorescent materials in the posterior pole. Spectral-domain OCT showed macular thinning with submacular fluid. The female patient had a concomitant macular edema associated with branched retinal vein occlusion in the left eye, which responded well to intravitreal bevacizumab injections. Genetic analysis demonstrated that both patients were compound heterozygous for one novel (Leu40Pro) and one previously identified (Ala195Val) *BEST1* variant. HEK293T cells transfected with the identified *BEST1* mutant showed significantly small currents compared to those transfected with the wild-type gene, whereas cells cotransfected with mutant and wild-type *BEST1* showed good chloride conductance. Cellular localization of *BEST1* was well conserved to the plasma membrane in the mutants.

CONCLUSIONS. We have identified and described the phenotype and in vitro functional aspects of a new *BEST1* mutation causing ARB. Clinically suspected ARB cases warrant genetic confirmation to confirm the diagnosis.

Keywords: *BEST1*, autosomal recessive bestrophinopathy, visual loss, retinal dystrophy

Investigative Ophthalmology & Visual Science

The bestrophin-1 (*BEST1*, also known as *VMD2*) gene is located on chromosome 11q13 and encodes a transmembrane protein consisting of 585 amino acids located on the basolateral membrane of retinal pigment epithelial (RPE) cells (Supplementary Fig. S1).[1,2] Although the exact function of *BEST1* is still not clear, it is generally believed to act as a chloride ion channel and has been shown to regulate voltage-gated Ca^{2+} channels in RPE cells, thus possibly having a dual function as a channel and a channel regulator.[1,2] The *BEST1* gene is expressed predominantly in RPE cells, and a mutation of this gene can generate a variety of ocular diseases with a broad phenotypic spectrum, which are now collectively referred to as bestrophinopathies. To date, five major categories of such diseases have been classified,[2,3] among which Best vitelliform macular dystrophy (VMD, Online Mendelian Inheritance in Man [OMIM] 153700), or Best disease, is the first and perhaps most

widely known.[4,5] Other diseases in this family include adult-onset vitelliform macular dystrophy (AVMD, OMIM 608161), autosomal dominant vitreoretinochoroidopathy (ADVIRC, OMIM 193220), retinitis pigmentosa 50 (RP50, OMIM 613194), and autosomal recessive bestrophinopathy (ARB; OMIM 611809).

Schatz et al.[6] published the first report of ARB patients with a compound *BEST1* heterozygous mutation in 2006. However, since the *BEST1* mutation was believed to segregate only in an autosomal dominant manner, they referred to this condition as a "variant phenotype" of Best disease, and speculated that the first mutation had a modifier effect on the second mutation. In 2008, Burgess et al.[7] defined this condition as a distinct category of bestrophinopathy and coined the term autosomal recessive bestrophinopathy. Unlike the situation with Best disease, no patient with ARB has been shown to demonstrate

vitelliform lesions in a typical "egg yolk" shape in the center of the macula; rather, the main characteristics of ARB are multifocal vitelliform lesions with subretinal fluid or macular edema.[2,6–13] Other associated clinical features of ARB include hyperopia, a shallow anterior chamber, and increased incidence of angle-closure glaucoma.[7,9,12] Electrophysiology tests tend to demonstrate normal or abnormal eletroretinogram (ERG) with absent light rise in electrooculogram (EOG). Although interest in ARB has been increasing recently, much remains to be discovered about the spectrum of symptoms and clinical variability of ARB phenotypes.

More than 100 Best disease variants and 20 ARB variants in *BEST1* have been reported so far[12–15] (http://www-huge.uni-regensburg.de/BEST1_database [in the public domain]; Supplementary Fig. S1). Some of the Best disease mutations were shown to act in a dominant-negative manner by severely reducing wild-type whole-cell currents when coexpressed in HEK293 cells with wild-type isoform.[16–18] Similarly, Burgess et al.[7] carried out whole-cell patch clamping of HEK293 cells transfected with their newly found ARB alleles with recessive mutation and showed that, in contrast to Best disease mutations, cotransfection with wild-type *BEST1* did not weaken the activity of wild-type *BEST1*, consistent with recessive features of a patient.

In this article, we present the results of a clinical, genetic, and in vitro electrophysiological investigation of a family with ARB. Whole-cell patch clamping of ARB alleles was conducted to confirm that a newly identified mutation leads to altered *BEST1* function in a recessive manner.

MATERIALS AND METHODS

Clinical Investigation

This study was approved by the Institutional Review Board of the Yonsei University College of Medicine and adhered to the tenets of the Declaration of Helsinki. Informed consent was obtained from all subjects prior to conducting investigations. Two patients with ARB and four of their first- and second-degree relatives were included in the study (Fig. 1). Clinical investigations in patients included best-corrected visual acuity, slit-lamp examination, indirect ophthalmoscopy, fundus photography, fundus autofluorescence imaging, spectral-domain optical coherence tomography (OCT), fluorescein angiography and indocyanine green angiography, and full-field ERG and EOG. Full-field ERG and EOG were performed according to the guidelines of the International Society for Clinical Electrophysiology of Vision (www.iscev.org). The normal range of the Arden ratio of the EOG (ratio of the light peak to the dark trough) is more than 1.8 for our laboratory.

Genetic Analysis

Genomic DNA was isolated from the subjects' blood using QIAamp RNA Blood Mini Kit (Cat. No. 51106; QIAGEN, Hilden, Germany). Each exon of the whole *BEST1* gene was amplified from genomic DNA by polymerase chain reaction (PCR) using the intronic oligonucleotide primers and PCR conditions described previously.[19] Each PCR was performed using Maxime PCR PreMix (Cat. No. 25167; iNtRON Biotech, Seoul, Korea). The PCR products were analyzed by direct sequencing using an Applied Biosystems (ABI) 3730 DNA sequencer (ABI, Foster City, CA, USA).

Plasmids and Cell Culture

Human embryonic kidney 293T cells (HEK293T) and Hela cells were cultured in Dulbecco's modified Eagle's medium (DMEM)-HG (Invitrogen, Carlsbad, CA, USA) supplemented with 10% (vol/vol) fetal bovine serum, 100 U/mL penicillin, and 0.1 mg/mL streptomycin. The mammalian-expressible plasmids for human *BEST1* (h*BEST1*) were purchased from GeneCopoeia (clone ID: EX-Q0269-M02; Rockville, MD, USA). The cDNA of h*BEST1* was subcloned into a pCMV-myc(N) plasmid using PCR amplification. The h*BEST1* L40P, A195V, and W93C mutant plasmids were generated using PCR-based site-directed mutagenesis. Plasmids were transiently transfected into cells using Lipofectamine Plus (Invitrogen). For electrophysiological experiments, h*BEST1* plasmids without tags were transfected at a 9:1 ratio with a plasmid expressing green fluorescence protein (pEGFP-N1). For surface biotinylation, immunoblotting, and immunocytochemistry, h*BEST1* plasmids containing a Myc tag were used.

Electrophysiology in Cultured Cells

Anion channel activities were measured in HEK293T cells using the whole-cell patch-clamp techniques reported previously.[20,21] Briefly, cells were transferred into a bath mounted on a stage with an inverted microscope (IX-70; Olympus, Tokyo, Japan). Conventional whole-cell clamp was achieved by rupturing the patch membrane after forming a gigaseal. The bath solution was perfused at 5 mL/min. The voltage and current recordings were performed at room temperature (22–25°C). Patch pipettes with a free-tip resistance of approximately 2 to 5 MΩ were connected to the head stage of a patch-clamp amplifier (Axopatch-700B; Molecular Devices, Sunnyvale, CA, USA). pCLAMP software v. 10.2 and Digidata-1440A (Molecular Devices) were used to acquire data and apply command pulses. Silver chloride reference electrodes were connected to the bath via a 1.5% agar bridge containing 3 M KCl solution. Voltage and current traces were stored and analyzed using Clampfit v. 10.2 and Origin v. 8.0 (OriginLab Corp., Northampton, MA, USA). Currents were sampled at 5 kHz. All data were low pass filtered at 1 kHz.

The bath solution for the whole-cell patch clamp contained 146 mM N-methyl-D-glucamine-Cl (NMGD-Cl), 1 mM $CaCl_2$, 1 mM $MgCl_2$, 5 mM glucose, and 10 mM HEPES (pH 7.4). The pipette solution contained 148 mM NMDG-Cl, 1 mM $MgCl_2$, 3 mM MgATP, 10 mM HEPES, and 5 mM ethylene glycol tetraacetic acid (EGTA) (pH 7.2). The free Ca^{2+} concentrations of the buffer solutions were fixed to 1 μM by adjusting the Ca^{2+} chelator EGTA (5 mM) and $CaCl_2$ concentrations using WEBMAX-C software (http://www.stanford.edu/~cpatton/maxc.html [in the public domain]). The osmolarity of the bath solution was set to be 10 mOsm higher than that of the pipette solution by adding sorbitol to suppress the volume-activated anion channels. To determine the current–voltage (I-V) relationship, the clamp mode was shifted to voltage clamp mode, and the I-V curve was obtained by applying step pulses from −100 to 100 mV (voltage interval: 20 mV; duration: 2 seconds; holding potential: 0 mV). In some experiments, h*BEST1*-expressing HEK293T cells were subjected to 5-Nitro-2-(3-phenylpropylamino)benzoic Acid (NPPB) (100 μM, Sigma-Aldrich Corp., St. Louis, MO, USA).

Surface Biotinylation and Immunoblotting

Surface biotinylation and immunoblotting was performed as described previously.[22] Transfected HEK293T cells were washed three times with ice-cold phosphate-buffered saline (PBS). The cells were then treated with sulfo-NHS-SS-biotin-containing buffer (Pierce, Rockford, IL, USA) for 30 minutes to biotinylate the plasma membrane proteins. After biotinylation, the cells were washed with quenching buffer to remove the
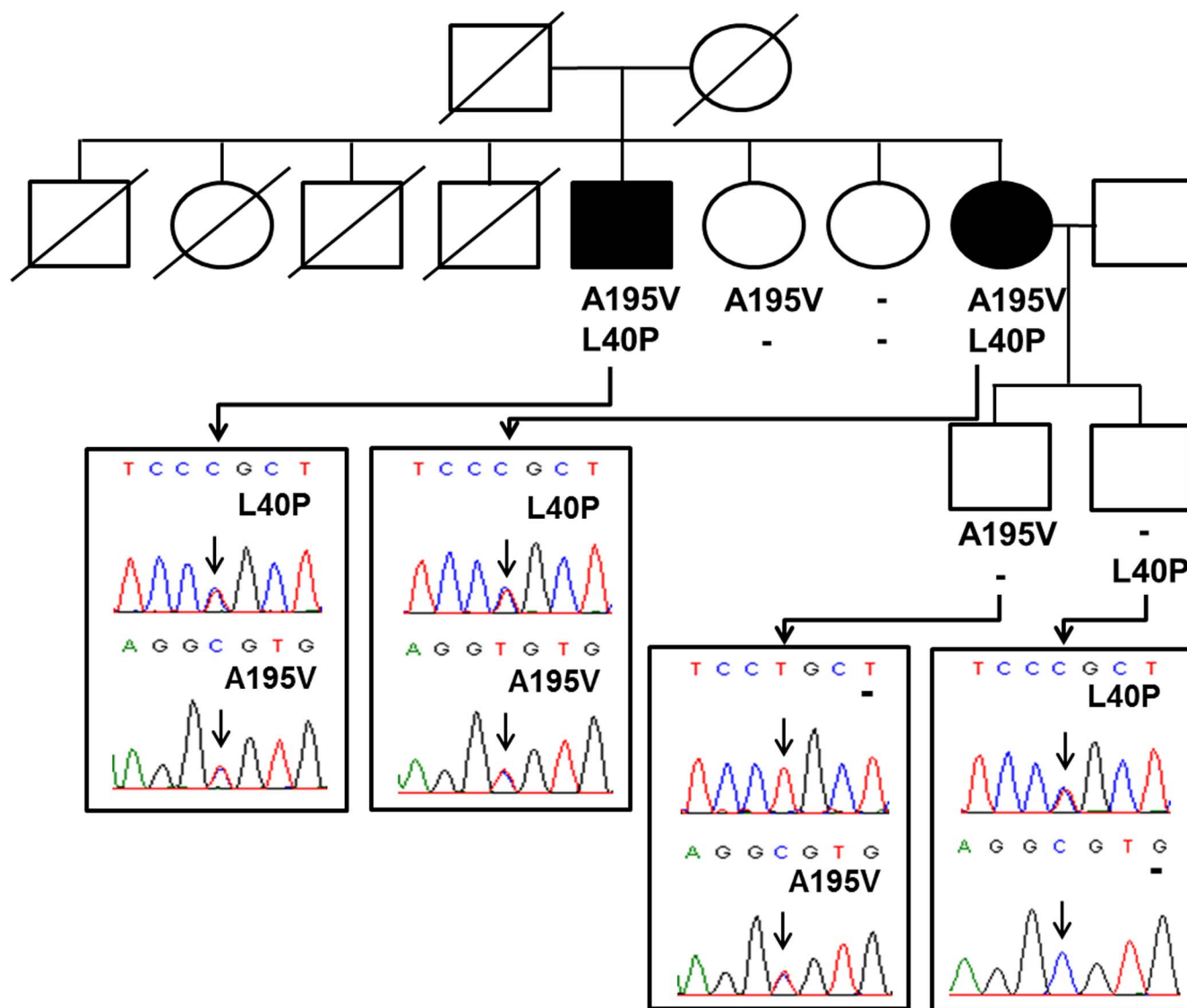
FIGURE 1. Pedigree of the family. Genetic screening of family members demonstrated two *BEST1* mutations in patients. Leu40Pro mutation has not been reported in previous studies and was identified as a novel mutation. The chromatograms of selected subjects are shown.

excess biotin and washed twice again with PBS. The cells were harvested and incubated overnight with avidin solution (Ultra-Link Immobilized NeutrAvidin Beads 10%, Pierce) at 4°C. Avidin-bound complexes were washed three times and the biotinylated proteins were eluted in a 2× sample buffer. The protein samples were suspended in a sodium dodecyl sulfate buffer and separated by sodium dodecyl sulfate–polyacrylamide gel electrophoresis. The separated proteins were transferred to a nitrocellulose membrane and blotted with appropriate primary and secondary antibodies. Anti-Myc (Santa Cruz Biotechnology, Santa Cruz, CA, USA) antibody was used as primary antibody, and anti-Mouse IgG Horseradish peroxidase (HRP) (Thermo Scientific, Rockford, IL, USA) antibody was used as secondary antibody. Protein bands were detected by enhanced chemiluminescence (Amersham Biosciences, Buckinghamshire, UK).

Immunocytochemistry

For immunocytochemistry, Hela cells were cultured on coverslips and immunostained 2 days after transfection. Cells grown on coverslips were fixed in 10% formalin for 10 minutes and permeabilized with 0.1% Triton X-100 for 10 minutes at room temperature. Nonspecific binding sites were blocked by incubation for 1 hour at room temperature with 0.1 mL PBS containing 5% horse serum, 1% bovine serum albumin, and 0.1% gelatin (blocking medium). After blocking, cells were stained by incubation with appropriate primary antibodies and then treated with fluorophore-tagged secondary antibodies. Fluorescent images were obtained with a Zeiss LSM 780 confocal microscope (Carl Zeiss, Berlin, Germany). Anti-myc (Santa Cruz Biotechnology), anti-calnexin, and anti-Na^+/K^+ pump (Abcam, Cambridge, MA, USA) were used as primary antibodies and purchased from commercial sources.

Statistical Analysis

The results are presented as means ± SEM. Statistical analysis was performed with analysis of variance (ANOVA) followed by Tukey's multiple comparison test as appropriate. $P < 0.05$ was considered statistically significant.

TABLE. Demography, Clinical Findings, and In Silico Analysis of the *BEST1* Mutations in a Family

Patient	Sex	Age at Onset, y	Age, y	Decimal Visual Acuity (Spherical Equivalent)		ERG		EOG, Arden Ratio		*BEST1* Mutations	Amino Acid Change	PolyPhen-2 Prediction	SIFT Prediction
				OD	OS	OD	OS	OD	OS				
1	M	25	66	0.05 (+3.00)	0.05 (+2.75)	WNL	WNL	1.0	1.0	**c.119T>C**	**L40P**	Probably damaging, **0.975**	Damaging, **0.011**
										c.584C>T	A195V	Probably damaging, 0.992	Damaging, 0.001
2	W	20	52	0.05 (+3.00)	0.02 (+3.25)	WNL	WNL	1.0	1.0	**c.119T>C**	**L40P**	Probably damaging, **0.975**	Damaging, **0.011**
										c.584C>T	A195V	Probably damaging, 0.992	Damaging, 0.001

Novel mutations in bold. M, man; W, woman; OD, right eye; OS, left eye; OU, both eyes; WNL, within normal limits; SIFT, sorts intolerant from tolerant.

RESULTS

Clinical Findings

The demographic and clinical details of the two related patients with ARB are summarized in the Table. Patient 1 was a 66-year-old man who reported significant central visual loss at the age of 25. His best-corrected visual acuity was 20/400 in both eyes at 66 years of age, which did not change during the follow-up of 2 years. The patient was hyperopic, and his intraocular pressure was within the normal range with no definite evidence of angle-closure glaucoma. The fundus showed bilateral symmetric RPE irregularity in the posterior pole with scattered punctate yellowish flecks (Fig. 2). These findings were more evident with autofluorescence imaging, which showed widespread variability of the autofluorescence. The OCT showed a disrupted outer retinal layer with serous macular detachments. Fluorescein angiography showed a patchy, mottled hyperfluorescent area in the affected lesion. Full-field ERG showed scotopic and photopic responses within the normal range. The EOG showed an absent light rise (Arden ratio, 1.0).

Patient 2 was a 52-year-old woman, the younger sister of patient 1. Like her brother, she noted significant visual loss in both eyes at the age of 20 years. She presented with a further decrease in her left eye visual acuity for 2 months. Her fundus findings were almost identical to those of patient 1, except for the recent development of branched retinal vein occlusion (BRVO) with macular edema in her left eye (Fig. 3). Her visual acuity was 20/400 in her right eye and 20/800 in her left eye. After two monthly intravitreal bevacizumab (1.25 mg/0.05 mL, respectively) injections, the macular edema in her left eye promptly resolved, but the serous macular detachment remained, which appeared similar to that of the fellow eye. Branched retinal vein occlusion did not recur during the follow-up of 2 years. Electrophysiology showed normal findings for the full-field ERG, but an absent EOG light rise (Arden ratio, 1.0) in both eyes. Her intraocular pressure was within the normal range and there was no clinical evidence of angle-closure glaucoma.

Genetic Findings

A Leu40Pro missense change and an Ala195Val missense change were detected in the *BEST1* gene of both patients 1 and 2. No other nonsynonymous mutation was found. The Leu40Pro mutation has not been previously reported in patients with either VMD or ARB. Among the eight siblings in the patients' family, blood samples of four deceased siblings along with the deceased parents could not be obtained for genetic analysis. One living sister had the Ala195Val mutation in one allele, and her phenotype was normal. Another sister had no mutation in the *BEST1* gene and had a normal phenotype.

One of two sons of patient 2 had the Leu40Pro mutation in one allele, and the other son of patient 2 had the Ala195Val mutation in one allele. The son with the Leu40Pro mutation had a normal phenotype, whereas the son with the Ala195Val mutation showed a focal hypopigmented RPE change in the right eye macula and a mottled orange placoid lesion in the left eye macula (Supplementary Fig. S2). This son had no ocular symptoms, with a visual acuity of 20/20 in both eyes. Full-field ERG and EOG findings were normal, and OCT findings were unremarkable for both lesions. The lesion size and characteristics did not change during the 2-year follow-up period.

In Vitro Study

Given the finding of one novel (Leu40Pro) and one previously reported (Ala195Val) variant of *BEST1* in the two related
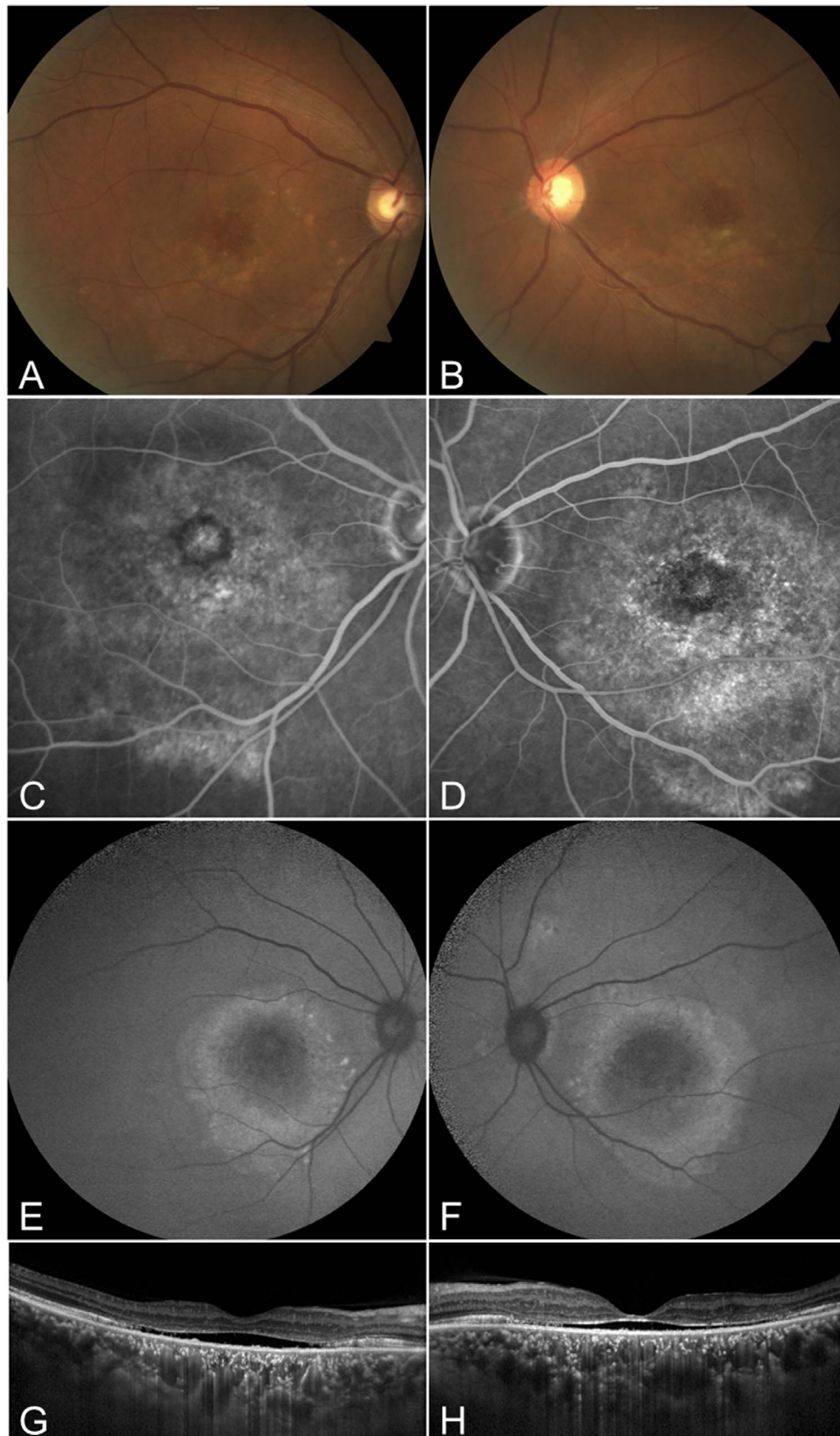
FIGURE 2. Clinical features of patient 1. A 66-year-old otherwise healthy man presented with reduced central vision in both eyes, which he first noticed when he was 25 years old. (A, B) Color fundus photographs showed bilateral, multifocal subretinal yellowish deposits and diffuse retinal pigment epithelial changes in the posterior pole in the right eye (A) and the left eye (B). (C, D) Corresponding lesions showed diffuse hyperfluorescence in the late-phase images of fluorescein angiography. (E, F) There are intense hyperautofluorescence of yellowish deposits and moderate hyperautofluorescence surrounding the macular lesions. (G, H) Horizontal spectral-domain optical coherence tomography images through fovea show retinal thinning, subretinal fluid, and the thickening of the choroidal layers.
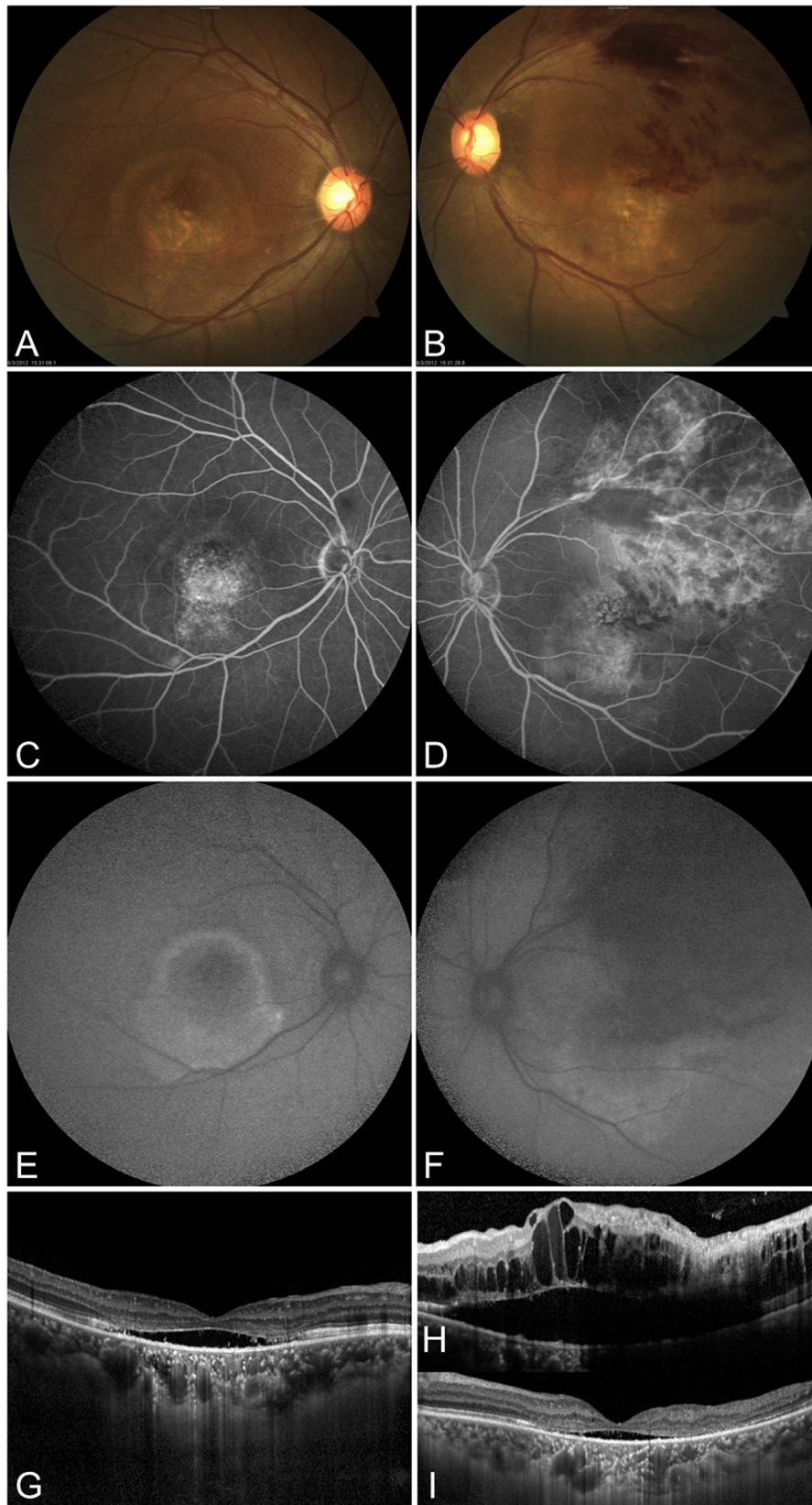
FIGURE 3. Clinical features of patient 2. A 52-year-old otherwise healthy woman presented with decreased visual acuity in her left eye. She had noticed reduced central vision in both eyes since she was 20 years old. (**A**, **B**) Color fundus photographs showed findings similar to those for her brother (Supplementary Fig. S2), but her left eye (**B**) showed the additional finding of flame-shaped retinal hemorrhage, a feature of branched retinal vein occlusion (BRVO). (**C**, **D**) Late-phase fluorescein angiography showed hyperfluorescence of the macular lesions and along superior arcade (**D**). (**E**, **F**) Yellowish deposits showed intense hyperautofluorescence and moderate hyperautofluorescence surrounding the macular lesions. There is a blockage of autofluorescence in the left eye (**F**) due to retinal hemorrhage. (**G**) Right eye optical coherence tomography (OCT) showed retinal

thinning, subretinal fluid, and thickened choroid. (**H**) Left eye OCT showed subretinal fluid and intraretinal fluid that are in part ascribed to copresent BRVO. (**I**) After two successive monthly intravitreal bevacizumab injections, left eye OCT image now looks similar to the right eye OCT image.

patients, we conducted further in vitro experiments to elucidate the potential functional defects resulting from these mutations. First, we examined the membrane expression of the mutant proteins. We transfected wild-type and mutant h*BEST1* clones into HEK293T cells or Hela cells and conducted a surface biotinylation assay, which can demonstrate the membrane expression of a protein selectively, and immunocytochemistry. All mutant and wild-type h*BEST1* proteins showed good membrane expression (Fig. 4A; Supplementary Figs. S3, S4). Next, we measured the calcium-activated currents using whole-cell patch recording of the human *BEST1* protein expressed in HEK293T cells (Figs. 4B–F; Supplementary Fig. S5). Similar to results from previous studies,[7] larger currents were observed in cells transfected with the wild-type plasmid compared to those observed in the mock-transfected HEK293T cells (Figs. 4B, 4C). And the currents were inhibited by NPPB, a chloride channel inhibitor, confirming that the measured currents are h*BEST1* chloride currents indeed (Supplementary Fig. S5). Furthermore, the currents observed in the cells transfected with the Leu40Pro and Ala195Val mutant plasmids were significantly smaller than those transfected with the wild type (Figs. 4D, 4E). These data indicate that the Leu40Pro and Ala195Val mutations significantly reduced *BEST1* function compared to that of the wild-type protein.

To evaluate whether the identified mutations show an evident autosomal recessive pattern, we cotransfected wild-type and mutant h*BEST1* plasmids to HEK293T cells and measured the current activity. As reported previously,[7,18,23] coexpression of Ala195Val mutant and wild-type *BEST1* resulted in activation of large currents (Fig. 5B), whereas coexpression of an autosomal dominant-type mutant, Trp93Cys, and the wild type resulted in activation of small currents (Fig. 5C). The novel mutation Leu40Pro showed autosomal recessive features similar to the Ala195Val mutant (Fig. 5A). Therefore, the Leu40Pro and Ala195Val mutations show an autosomal recessive pattern of inheritance, confirming the clinical data. To mimic the patients' condition, we measured the currents under coexpression of the Leu40Pro and Ala195Val mutants and confirmed that no current was generated (Fig. 5D). There was no significant difference in
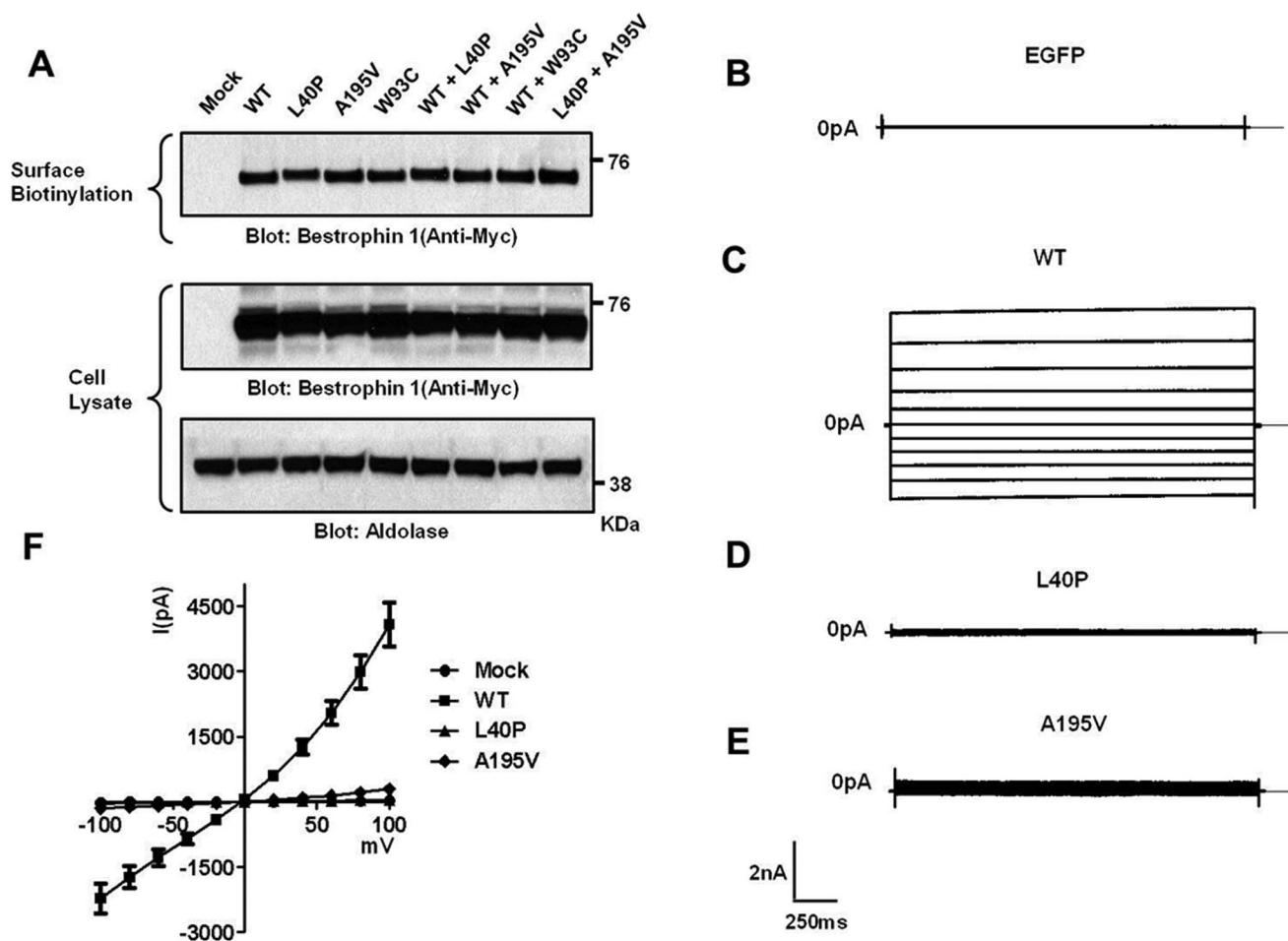

FIGURE 4. L40P and A195V mutant *BEST1* shows tiny currents in comparison with wild type. HEK293T cells were transfected with plasmids expressing wild-type and mutant h*BEST1*. (**A**) Surface biotinylation of h*BEST1*. Immunoblotting of transfected HEK293T cells using anti-Myc antibody. (**B–E**) Representative traces of HEK293T cells transfected with EGFP alone (**B**), wild type (**C**), Leu40Pro (**D**), or Ala195Val bestrophin-1 (**E**). Voltage was stepped from a holding potential of 0 mV to between −100 and +100 mV in 20-mV steps. Step duration was 2000 ms. (**F**) Current–voltage relationship of mock, wild-type, and mutant bestrophin-1. Data are presented as mean ± SEM.
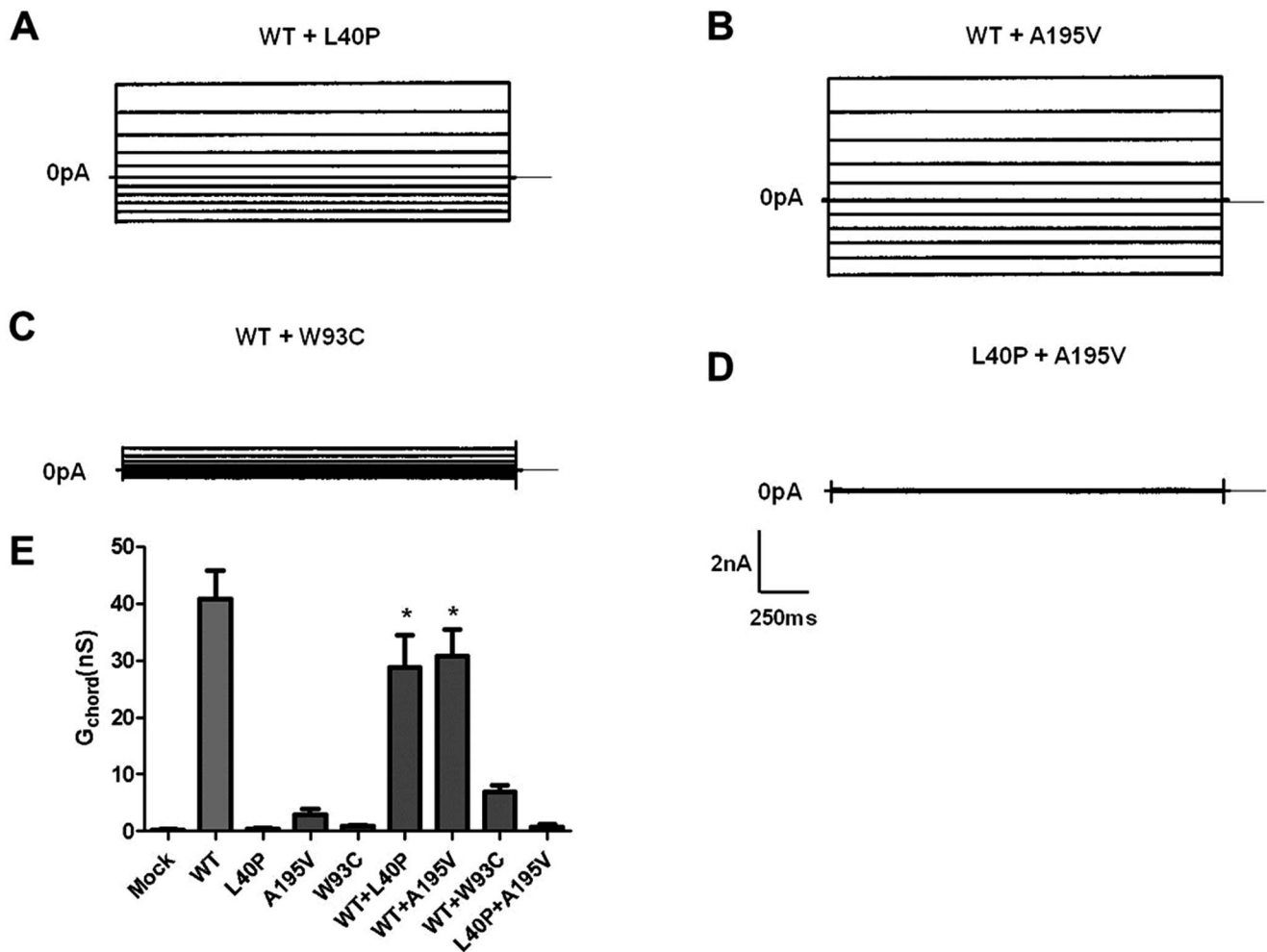
FIGURE 5. L40P and A195V bestrophin-1 shows autosomal recessive character. Plasmids expressing wild-type and each mutant bestrophin-1 were cotransfected to HEK293T cells. (**A–C**) Representative traces of HEK293T cells transiently transfected with wild-type bestrophin-1 plus either (**A**) Leu40Pro, (**B**) Ala195Val, or (**C**) Trp93Cys. (**D**) Representative traces of HEK293T cells transiently transfected with Leu40Pro and Ala195Val bestrophin-1. (**E**) The mean outward chord conductances (G_{chord}) in transfected HEK293 cells, calculated over 0 mV to +100 mV. *Not significant compared to wild type using ANOVA. Data are presented as mean ± SEM.

conductance between cells transfected with the wild type only and those cotransfected with the wild type and either the Leu40Pro or Ala195Val mutant (Fig. 5E).

DISCUSSION

Since it was first defined as a distinct type of bestrophinopathy in 2008,[7] there has been growing interest in ARB, with subsequent case series and reports that soon followed.[8–13,24–29] An important clinical component of ARB is its autosomal recessive nature with a *BEST1*-null phenotype, which makes it a potentially attractive candidate for gene replacement therapy.[12] Unlike ARB, most other diseases ascribed to *BEST1* mutations are autosomal dominantly inherited. We believe that ARB may not be as rare a disease as previously thought and is possibly easily misdiagnosed as other conditions such as chronic central serous chorioretinopathy, fundus flavimaculatus, Vogt-Koyanagi-Harada disease, and other types of vitelliform dystrophies.[13,30] With a high clinical index of suspicion, more cases with new mutations should be identified and reported.

It may be noteworthy that one of the sons of patient 2, who had the Ala195Val mutation in one allele, also had a hyper-autofluorescent macular lesion in one eye. This lesion did not appear to be a typical lesion that has been described for either autosomal dominant- or autosomal recessive-type bestrophinopathy. The patient was asymptomatic with normal ERG and EOG findings. The lesion has been followed up for 2 years, and so far there has been no change in its size or characteristics. This lesion may not be ascribed to the presence of the Ala195Val mutation in one allele, since one of the sisters of patient 2 also has the Ala195Val mutation in one allele but showed completely normal fundus findings. We could not find a previous study on the phenotypic changes associated with only the Ala195Val mutation of *BEST1*. Therefore, this lesion could be an incidental finding unrelated to ARB, although periodic follow-ups are planned to further investigate its nature. And one of our patients presented with concomitant BRVO with worsened cystoid macular edema in one eye, which promptly responded to intravitreal bevacizumab treatment (Fig. 3). However, we suspect that bevacizumab was successful in resolving the macular edema ascribed to BRVO only because

the subretinal fluid remained. To our knowledge, this is the first report of ARB associated with BRVO.

We conducted in vitro experiments to directly evaluate whether the novel variant of *BEST1* (Leu40Pro) is associated with physiological defects and is an autosomal recessive trait. Some autosomal recessive mutations of membrane proteins such as cystic fibrosis transmembrane conductance regulator (*CFTR*) and pendrin are related to protein misfolding, retention in the endoplasmic reticulum (ER), and ultimate degradation by the ER-associated degradation (ERAD) pathway.[22,31] Therefore, we examined the membrane expression of the h*BEST1* mutant using a surface biotinylation assay and immunocytochemistry, and found no defect on the membrane localization of *BEST1*. These results suggest that the Leu40Pro mutation is associated with defects to current activation rather than protein expression.

We therefore evaluated the current activation of the h*BEST1* mutants by patch-clamp recording. The Leu40Pro mutant did not generate calcium-activated currents, whereas the wild type generated large currents. Furthermore, the Leu40Pro mutant showed autosomal recessive features in cells cotransfected with the wild-type gene, confirming previous findings. The Leu41Pro mutant was reported as autosomal recessive previously.[7,18] This adjacent autosomal recessive-type mutant data support an autosomal recessive inheritance pattern of the Leu40Pro mutant. To simulate the patients' compound heterozygous mutations, cotransfection of Leu40-Pro and Ala195Val mutant plasmids in HEK293T cells was performed. No current was generated in the cotransfected cells, suggesting that the Leu40Pro mutation causes ARB in both homozygous and compound heterozygous patterns.

In conclusion, we conducted a comprehensive clinical and molecular evaluation of an ARB family with a compound heterozygous mutation in *BEST1*. An in vitro functional experiment confirmed the autosomal recessive nature of the Leu40Pro mutation. The ARB of one of the patients was complicated with BRVO-associated macular edema, which was successfully managed with intravitreal bevacizumab injections. The autosomal recessive nature and clinical features that mimic other more common macular diseases indicate that clinically suspected cases of ARB warrant genetic confirmation to confirm the diagnosis.

References

1. Boon CJ, Klevering BJ, Leroy BP, Hoyng CB, Keunen JE, den Hollander AI. The spectrum of ocular phenotypes caused by mutations in the BEST1 gene. *Prog Retin Eye Res*. 2009;28:187–205.

2. Pasquay C, Wang LF, Lorenz B, Preising MN. Bestrophin 1–phenotypes and functional aspects in bestrophinopathies. *Ophthalmic Genet*. 2015;36:193–212.

3. Davidson AE, Millar ID, Urquhart JE, et al. Missense mutations in a retinal pigment epithelium protein, bestrophin-1, cause retinitis pigmentosa. *Am J Hum Genet*. 2009;85:581–592.

4. Best F. Uber eine hereditare Maculaaffektion. *Z Augenheilk*. 1905;199–212.

5. Petrukhin K, Koisti MJ, Bakall B, et al. Identification of the gene responsible for Best macular dystrophy. *Nat Genet*. 1998; 19:241–247.

6. Schatz P, Klar J, Andreasson S, Ponjavic V, Dahl N. Variant phenotype of Best vitelliform macular dystrophy associated with compound heterozygous mutations in VMD2. *Ophthalmic Genet*. 2006;27:51–56.

7. Burgess R, Millar ID, Leroy BP, et al. Biallelic mutation of BEST1 causes a distinct retinopathy in humans. *Am J Hum Genet*. 2008;82:19–31.

8. Sharon D, Al-Hamdani S, Engelsberg K, et al. Ocular phenotype analysis of a family with biallelic mutations in the BEST1 gene. *Am J Ophthalmol*. 2014;157:697–709, e691.

9. Pomares E, Bures-Jelstrup A, Ruiz-Nogales S, Corcostegui B, Gonzalez-Duarte R, Navarro R. Nonsense-mediated decay as the molecular cause for autosomal recessive bestrophinopathy in two unrelated families. *Invest Ophthalmol Vis Sci*. 2012;53: 532–537.

10. MacDonald IM, Gudiseva HV, Villanueva A, Greve M, Caruso R, Ayyagari R. Phenotype and genotype of patients with autosomal recessive bestrophinopathy. *Ophthalmic Genet*. 2012;33:123–129.

11. Guerriero S, Preising MN, Ciccolella N, Causio F, Lorenz B, Fischetto R. Autosomal recessive bestrophinopathy: new observations on the retinal phenotype - clinical and molecular report of an Italian family. *Ophthalmologica*. 2011;225:228–235.

12. Boon CJ, van den Born LI, Visser L, et al. Autosomal recessive bestrophinopathy: differential diagnosis and treatment options. *Ophthalmology*. 2013;120:809–820.

13. Fung AT, Yzer S, Goldberg N, et al. New Best1 mutations in autosomal recessive bestrophinopathy. *Retina*. 2015;35:773–782.

14. Pomares E, Burés Jelstrup A, Ruiz Nogales S, Corcóstegui B, González Duarte R, Navarro R. Nonsense-mediated decay as the molecular cause for autosomal recessive bestrophinopathy in two unrelated families. *Invest Ophthalmol Vis Sci*. 2012;53: 532–537.

15. Cascavilla ML, Querques G, Stenirri S, Battaglia Parodi M, Querques L, Bandello F. Unilateral vitelliform phenotype in autosomal recessive bestrophinopathy. *Ophthalmic Res*. 2012; 48:146–150.

16. Sun H, Tsunenari T, Yau K, Nathans J. The vitelliform macular dystrophy protein defines a new family of chloride channels. *Proc Natl Acad Sci U S A*. 2002;99:4008–4013.

17. Qu Z, Wei RW, Mann W, Hartzell HC. Two bestrophins cloned from Xenopus laevis oocytes express Ca(2+)-activated Cl(-) currents. *J Biol Chem*. 2003;278:49563–49572.

18. Davidson AE, Millar ID, Burgess Mullan R, et al. Functional characterization of bestrophin-1 missense mutations associated with autosomal recessive bestrophinopathy. *Invest Ophthalmol Vis Sci*. 2011;52:3730–3736.

19. Lacassagne E, Dhuez A, Rigaudiere F, et al. Phenotypic variability in a French family with a novel mutation in the BEST1 gene causing multifocal best vitelliform macular dystrophy. *Mol Vis*. 2011;17:309–322.

20. Park HW, Nam JH, Kim JY, et al. Dynamic regulation of CFTR bicarbonate permeability by [Cl-]i and its role in pancreatic bicarbonate secretion. *Gastroenterology*. 2010;139:620–631.

21. Jung J, Nam JH, Park HW, Oh U, Yoon J, Lee MG. Dynamic modulation of ANO1/TMEM16A HCO3(-) permeability by Ca2+/calmodulin. *Proc Natl Acad Sci U S A*. 2013;110:360–365.

22. Gee HY, Noh SH, Tang BL, Kim KH, Lee MG. Rescue of ΔF508-CFTR trafficking via a GRASP-dependent unconventional secretion pathway. *Cell*. 2011;146:746–760.

23. Kinnick TR, Mullins RF, Dev S, et al. Autosomal recessive vitelliform macular dystrophy in a large cohort of vitelliform macular dystrophy patients. *Retina*. 2011;31:581–595.

24. Gerth C, Zawadzki RJ, Werner JS, Heon E. Detailed analysis of retinal function and morphology in a patient with autosomal recessive bestrophinopathy (ARB). *Doc Ophthalmol*. 2009; 118:239–246.

25. Crowley C, Paterson R, Lamey T, et al. Autosomal recessive bestrophinopathy associated with angle-closure glaucoma. *Doc Ophthalmol*. 2014;129:57–63.

26. Borman AD, Davidson AE, O'Sullivan J, et al. Childhood-onset autosomal recessive bestrophinopathy. *Arch Ophthalmol*. 2011;129:1088–1093.

27. Davidson AE, Sergouniotis PI, Burgess-Mullan R, et al. A synonymous codon variant in two patients with autosomal recessive bestrophinopathy alters in vitro splicing of BEST1. *Mol Vis*. 2010;16:2916–2922.

28. Pineiro-Gallego T, Alvarez M, Pereiro I, et al. Clinical evaluation of two consanguineous families with homozygous mutations in BEST1. *Mol Vis*. 2011;17:1607–1617.

29. Zhao L, Grob S, Corey R, et al. A novel compound heterozygous mutation in the BEST1 gene causes autosomal recessive Best vitelliform macular dystrophy. *Eye (Lond)*. 2012;26:866–871.

30. Fung A, Yzer S, Allikmets R. Clinical and genetic misdiagnosis of autosomal recessive bestrophinopathy. *JAMA Ophthalmol*. 2013;131:1651.

31. Yoon JS, Park HJ, Yoo SY, et al. Heterogeneity in the processing defect of SLC26A4 mutants. *J Med Genet*. 2008;45:411–419.